Nuclear Electric-Field Gradient Determination Utilizing the Mössbauer Effect (Fe⁵⁷)*

PETER ZORY†‡

Carnegie Institute of Technology, Pittsburgh, Pennsylvania

(Received 7 June 1965)

If a compound containing Fe⁵⁷ exhibits a two-line Mössbauer absorption spectrum, as is the case for most paramagnetic ferrous salts, then this spectrum may usually be attributed to the electrostatic interaction between an electric-field gradient (EFG) and the quadrupole moment of the first excited state of the Fe⁵⁷. Since the EFG may be represented as a traceless, symmetric tensor of the second rank, it is completely specified by five independent parameters. If the absorber is a single crystal, the two absorption peaks will generally have different intensities, the ratio of the intensities depending upon the orientation of the incident, unpolarized radiation relative to the crystal axes. In this paper, a general method is developed which utilizes this intensity ratio to determine the five EFG parameters. The possibility of an anisotropic recoilless factor is also considered. The method is then applied to $FeCl_2 \cdot 4H_2O$.

1. INTRODUCTION

A NUCLEUS with spin angular momentum $I \geq 1$, in the presence of an electric-field gradient (EFG), may have the degeneracy of its $(2I+1)$ spin-orientation levels partially removed by the electrostatic interaction of its quadrupole moment with the EFG.[1] Since the EFG may be represented as a traceless, symmetric tensor of the second rank, it is completely specified by five independent parameters. Three of these parameters locate the principal axes of the EFG relative to the atomic environment or crystal axes. If the nuclear environment is of sufficiently low symmetry, then the orientation of these principal axes is not obvious and must be determined by experiment. For nuclei possessing quadrupole moments in their ground state, methods utilizing nuclear quadrupole resonance have been developed to determine these orientation parameters.[2] This paper will be concerned primarily with indicating how the Mössbauer effect[3] may be utilized to determine these same parameters for nuclear excited states, using as an illustration, the quadrupole interaction of the first excited state of Fe⁵⁷ in the crystal $FeCl_2 \cdot 4H_2O$. Our method takes advantage of the anisotropy of the dipole γ emission (or absorption) relative to the orientation of the nuclear spin, which is in turn related to the principal axes of the EFG.

2. EXPERIMENTAL OBSERVATIONS

Mössbauer resonance absorption, utilizing the 14.4-keV transition between the ground and first excited states of Fe⁵⁷, has been observed in numerous para-

magnetic ferrous compounds.[4] If one uses a monoenergetic unpolarized source, e.g., Co⁵⁷ in Cu or Cr, in conjunction with the ferrous salt as the absorber, the measured spectrum is usually characterized by two absorption peaks. Since the ground state has no quadrupole moment, the observed splitting, generally ranging from 20 to 40 Mc/sec, is attributed to an electrostatic interaction between the quadrupole moment of the first excited state and the EFG produced by the electrons and ions surrounding the nucleus. Since the Fe⁵⁷ first excited state has spin $\frac{3}{2}$, the Hamiltonian for the interaction, written in the principal-axis system of the EFG is[5]

$$H_Q = \tfrac{1}{4}e^2qQ[I_z^2 - \tfrac{5}{4} + \tfrac{1}{6}\eta(I_+^2 + I_-^2)] \qquad (1a)$$

with eigenvalues

$$E_3 = \pm \tfrac{1}{4}e^2qQ(1 + \tfrac{1}{3}\eta^2)^{1/2}, \qquad (1b)$$

where

$[\hat{x}\hat{y}\hat{z}]$ = principal axes of EFG ($\hat{z}$ = major axis),

$\quad eq$ = EFG in $\hat{z}$ direction = V_{zz},

$\quad \eta$ = asymmetry about $\hat{z}$ ($0 \leq \eta < 1$),

$\quad Q$ = quadrupole moment of the first excited state of Fe⁵⁷.

In future discussion, we shall use the designations "3" and "1" to indicate absorptive transitions to the levels with hyperfine energies E_3 and E_1, respectively, these energies being defined in Eq. (1b).[6]

Using powdered absorbers, the intensities of the two peaks are usually of the same order of magnitude although this need not be true if the anisotropy in the Lamb-Mössbauer recoilless factor is significant.[7] Differences in peak intensities may also arise from various

¹ A. Abragam, *The Principles of Nuclear Magnetism* (Clarendon Press, Oxford, England, 1961), Chap. VI.

² T. P. Das and E. L. Hahn, *Solid State Physics*, edited by F. Seitz and D. Turnbull (Academic Press Inc., New York, 1958), Suppl. 1.

³ H. Frauenfelder, *The Mössbauer Effect* (W. A. Benjamin and Company, Inc., New York, 1962).

⁴ S. DeBenedetti, G. Lang, and R. Ingalls, Phys. Rev. Letters 6, 60 (1961).

⁵ M. H. Cohen and F. Reif, *Solid State Physics* (Academic Press Inc., New York, 1957), Vol. 5.

⁶ The transition to level "3" will have less energy than the transition to level "1" if e^2qQ is negative.

⁷ V. I. Goldanskii, E. F. Makarov, and V. V. Khrapov, Phys. Letters 3, 344 (1963).
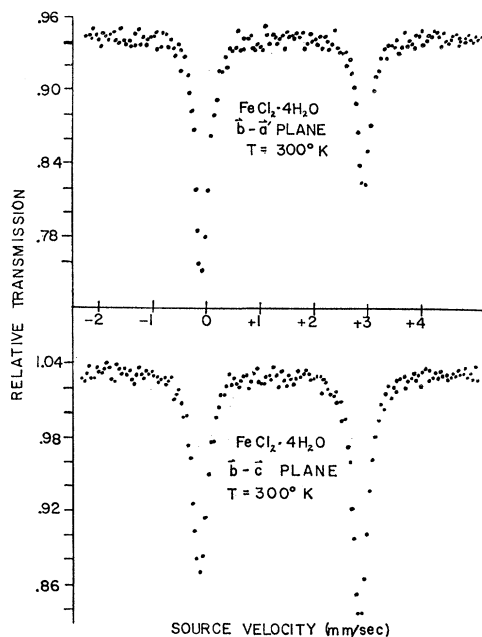
FIG. 1. Observed absorption spectra when unpolarized source radiation is incident on crystal: (upper)—parallel to c axis, (lower)—parallel to a′ axis.

relaxation mechanisms,[8] although these are probably important only in crystals with a dilute concentration of ferrous ions. If one employs single crystals as absorbers, the two peak intensities will in general be quite different, varying in a complicated way with the crystal orientation relative to the incident photon beam. Figure 1 shows two typical experimental spectra for a single crystal of $FeCl_2 \cdot 4H_2O$. The upper spectrum is observed when the source radiation is parallel to the c axis of the crystal, the lower spectrum being observed when the radiation is perpendicular to c. These experimental data were obtained using a standard velocity sweep arrangement in which the sinusoidal velocity signal generated by the source motion is fed directly to the analog to digital converter of a multichannel analyzer.

3. ABSORPTION AREAS

In order to determine the EFG parameters from data of this type, the experimental quantities to be utilized are the absorption peak areas. If we assume that we have a monochromatic, unpolarized source and a single-crystal absorber with one absorbing nucleus per unit cell, it may be shown[9] that the area under the nth absorption is approximately proportional to

$$\alpha_n \approx \int_0^\infty dE(1-\exp[\sigma_n(E,\theta,\phi)f'(\theta,\phi)Nt]), \quad (2)$$

[8] M. Blume, Phys. Rev. Letters 14, 96 (1965).
[9] G. Lang, Nucl. Instr. Methods 24, 425 (1963).

where

$\sigma_n(E,\theta,\phi) \equiv$ the energy-dependent cross section per nucleus for transition n when the incident, unpolarized beam makes polar and azimuthal angles θ and ϕ relative to the perturbing fields causing the splitting,

$f'(\theta,\phi) \equiv$ recoilless absorption probability whose angular dependence derives from the anisotropy in the mean square displacement of the vibrating nucleus,

$N =$ volume density of nuclei capable of resonance absorption,

$t =$ sample thickness.

Assuming that the quantity $\sigma_n(E_n,\theta,\phi)f'(\theta,\phi)Nt \ll 1$, the exponential may be expanded and the expression for the area reduces to

$$\alpha_n \sim Ntf'(\theta,\phi)\int_0^\infty \sigma_n(E,\theta,\phi)dE. \quad (3)$$

It may be shown from considerations in Chap. IV of Ref. 10 that,

$$\sigma_n(E,\theta,\phi) \sim \lambda^2 A_n(\theta,\phi)k(E-E_n),$$

where

$\lambda =$ unperturbed gamma wavelength,

$A_n(\theta,\phi)d\Omega =$ the spontaneous-transition probability for *emitting a photon* with energy E_n into solid angle $d\Omega$ at (θ,ϕ),

$k(E-E_n) =$ a Lorentzian function normalized so that

$$\int_0^\infty k(E-E_n)dE = 1.$$

Using a semiclassical approach, which is sufficient for our purposes, and restricting discussion to either pure electric- or magnetic-dipole radiation, it can be shown that $A_n(\theta,\phi)$ is given by[11]

$$A_n(\theta,\phi) \sim E_n^3(|\hat{\theta}\cdot D_n|^2 + |\hat{\phi}\cdot D_n|^2) \equiv E_n^3 p_n(\theta,\phi), \quad (4)$$

where $\hat{\theta}$ and $\hat{\phi}$ are the spherical unit vectors and D_n is the matrix element of the nuclear dipole-moment operator which interacts with the radiation field. If the radiation is pure electric-dipole, then $D_n = P_n$, the matrix element of the nuclear electric-dipole moment; if the radiation is pure magnetic-dipole, then $D_n = M_n$, the matrix element of the nuclear magnetic-dipole moment. The quantity $p_n(\theta,\phi)$, defined in (4), we shall call the

[10] E. U. Condon and G. H. Shortley, *The Theory of Atomic Spectra* (The Macmillan Company, New York, 1935).
[11] Equation 5⁴4 of Ref. 10 is a classica expression containing those terms in the radial component of the time-averaged Poynting vector $\langle S \rangle_r$, which contribute at large distance to the power integral $\int_{4\pi}\langle S \rangle_r r^2 d\Omega$. It is easily shown that Eq. 5⁴4 is equivalent to $\langle S \rangle_r = (ck^4/8\pi r^2)|(\hat{\theta}\cdot D)\hat{\theta} + (\hat{\phi}\cdot D)\hat{\phi}|^2$ and that it is valid for either electric, $D = P$, or magnetic, $D = M$, dipole radiation. It is transformed to the correct quantum-mechanical formula by replacing the classical dipole-moment operator D by twice the matrix element of $D \equiv D_n$.

relative angular dependent absorption probability for transition n. Substituting these results into (3), we obtain

$$\mathcal{C}_n \sim N t \lambda^2 E_n{}^3 f'(\theta,\phi) p_n(\theta,\phi).$$

We shall be interested in taking ratios of areas and therefore ratios of the type $(E_n/E_m)^3$ will occur. For all practical purposes these are all equal to 1 since the gamma-ray energy is very much greater than the hyperfine-splitting energy. Consequently, the expression for the area under the nth absorption peak reduces to

$$\mathcal{C}_n \sim f'(\theta,\phi) p(\theta,\phi). \tag{5}$$

In order to utilize (5) effectively, it is necessary to have some knowledge of the crystal under investigation. If the crystal has only one absorbing nucleus per unit cell, then the ratio of the areas for transitions n and m is given simply by the ratio of the relative absorption probabilities. If the crystal has two or more equivalent sites per unit cell (equivalent in the sense that the surroundings of the absorbing nuclei are the same but differ in orientation), then the ratio of the areas is given by

$$\frac{\mathcal{C}_n}{\mathcal{C}_m} = \frac{\sum\limits_{i}^{\text{sites}} p_n(\theta_i,\phi_i) f'(\theta_i,\phi_i)}{\sum\limits_{i} p_m(\theta_i,\phi_i) f'(\theta_i,\phi_i)}. \tag{6}$$

Crystals having inequivalent nuclear sites in the unit cell produce multiple-line spectra and the only new problem comes in grouping the lines according to the site from which they originate.

It is interesting to note, if the absorber is a powder, that is, if all possible orientations of the fields relative to the incident beam are present in the absorber, then the correct expression for the ratio of the areas is given by

$$\frac{\mathcal{C}_n}{\mathcal{C}_m} = \frac{\displaystyle\int_{4\pi} p_n(\theta,\phi) f'(\theta,\phi) d\Omega}{\displaystyle\int_{4\pi} p_m(\theta,\phi) f'(\theta,\phi) d\Omega}. \tag{7}$$

The possibility that the angular dependence of the f' factor could be important in determining the relative intensities of Mössbauer absorption lines in powdered absorbers was first noted in a paper by V. I. Goldanskii et al.[7]

This discussion having to do with absorption areas is quite general and may be applied to "any" Mössbauer single-crystal experiment (where the Mössbauer radiation is pure electric- or magnetic-dipole). However, we are interested here in determining the EFG parameters at an Fe^{57} nucleus and since there are only two absorption peaks, relative absorption probabilities p_3 and p_1, there is only one area ratio of interest, viz., $\mathcal{C}_3/\mathcal{C}_1$. Since
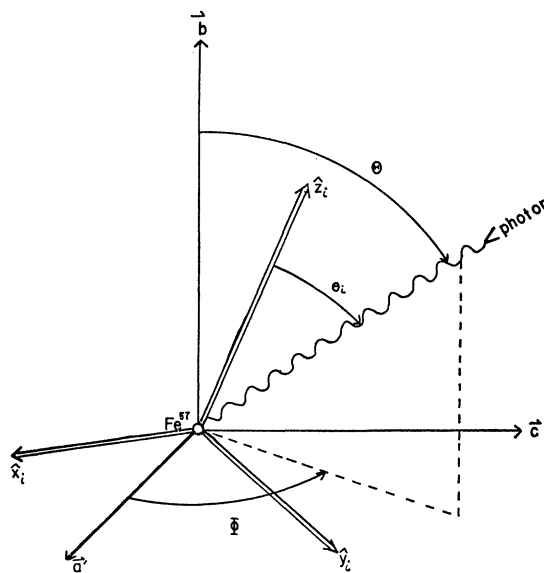
FIG. 2. Schematic of the absorption process indicating the orientation of the incident photon beam; relative to the crystal axes (a′,b,c) and relative to the EFG principal axes ($\hat{x}_i,\hat{y}_i,\hat{z}_i$) of the ith site in the unit cell.

the $FeCl_2 \cdot 4H_2O$ crystal contains two equivalent sites per unit cell, Eq. (6) is the appropriate equation for analyzing the experimental data. In order to be useful however, Eq. (6) must be re-expressed in terms of the unknown nuclear EFG parameters.

4. AREA RATIO FOR $FeCl_2 \cdot 4H_2O$

In re-expressing Eq. (6), we begin first by describing the $FeCl_2 \cdot 4H_2O$ crystal. Ferrous chloride tetrahydrate is a monoclinic crystal, space group $P2_1/c$, with unit cell dimensions $a = 5.91$, $b = 7.17$, $c = 8.44$ Å, the axes a and c making an angle of $112° 10'$.[12] The basic structural unit of the crystal consists of an Fe^{++} ion surrounded by a distorted octahedron constructed from two chlorine ions and four water molecules. The unit cell of the crystal is composed of two of these octahedra, the operation transforming one into the other being a rotation of $180°$ about $\mathbf{b}$.[13]

Figure 2 clarifies the experimental situation. Since the crystal axes $\mathbf{a}$, $\mathbf{b}$, and $\mathbf{c}$ are not orthogonal, it is convenient to introduce an axis $\mathbf{a}'$, constructed so that the axes $\mathbf{a}'$, $\mathbf{b}$, and $\mathbf{c}$ are mutually orthogonal. The angles Θ, Φ are then the orientation angles of the incident radiation relative to (a′,b,c). The unit vectors ($\hat{x}_i,\hat{y}_i,\hat{z}_i$) locate the EFG principal axes of the ith site, the three Euler angles ($\alpha_i,\beta_i,\gamma_i$), designating their orientation relative to (a′,b,c) being unknown. The angles θ_i, ϕ_i are the orientation angles of the incident radiation relative to ($\hat{x}_i,\hat{y}_i,\hat{z}_i$).

[12] B. R. Penfold and J. A. Grigor, Acta Cryst. 12, 850 (1959).

[13] We are disregarding translation operations since only the orientation of the sites relative to the crystal axes is important in the experiment.

By utilizing the fact that the Fe^{57}, 14.4-keV transition is magnetic-dipole,[14] it can be shown that the relative absorption probabilities, p_3 and p_1, which are to be substituted into Eq. (6) are given by (see Appendix A)

$$p_3(\theta,\phi)=4[(3+\eta^2)/3]^{1/2}$$
$$+(3\cos^2\theta-1+\eta\sin^2\theta\cos2\phi),$$
$$p_1(\theta,\phi)=4[(3+\eta^2)/3]^{1/2} \qquad (8)$$
$$-(3\cos^2\theta-1+\eta\sin^2\theta\cos2\phi).$$

We are interested first in finding expressions for $\cos^2\theta_i$ and $\sin^2\theta_i(\cos^2\phi_i-\sin^2\phi_i)$ in terms of the known experimental angles Θ, Φ and the unknown Euler angles relating site i to axes $(\hat{a}'\hat{b}\hat{c})$.

Now it is easily shown that

$$\sin\theta_i\cos\phi_i=\sin\Theta\cos\Phi(\hat{a}'\cdot\hat{x}_i)$$
$$+\sin\Theta\sin\Phi(\hat{c}\cdot\hat{x}_i)+\cos\Theta(\hat{b}\cdot\hat{x}_i),$$
$$\sin\theta_i\sin\phi_i=\sin\Theta\cos\Phi(\hat{a}'\cdot\hat{y}_i)$$
$$+\sin\Theta\sin\Phi(\hat{c}\cdot\hat{y}_i)+\cos\Theta(\hat{b}\cdot\hat{y}_i), \qquad (9)$$
$$\cos\theta_i=\sin\Theta\cos\Phi(\hat{a}'\cdot\hat{z}_i)$$
$$+\sin\Theta\sin\Phi(\hat{c}\cdot\hat{z}_i)+\cos\Theta(\hat{b}\cdot\hat{z}_i).$$

Each of the direction cosines, i.e., $\hat{a}'\cdot\hat{x}_i$, $\hat{c}\cdot\hat{y}_i$, etc., can be expressed as a function of the same Euler angles, $\alpha_i, \beta_i, \gamma_i$.[15]

If we let $\hat{k}_i$ stand for either $\hat{x}_i$, $\hat{y}_i$, or $\hat{z}_i$, then the symmetry relation between the two sites, i.e., the 180° rotation about the **b** axis, can be written as

$$\hat{a}'\cdot\hat{k}_1=-\hat{a}'\cdot\hat{k}_2,$$
$$\hat{c}\cdot\hat{k}_1=-\hat{c}\cdot\hat{k}_2, \qquad (10)$$
$$\hat{b}\cdot\hat{k}_1=\hat{b}\cdot\hat{k}_2.$$

Consequently, if we assume that f' is isotropic, then by utilizing Eqs. (8), (9), and (10), it may be shown that Eq. (6) for $FeCl_2\cdot4H_2O$ has the form

$$\frac{\alpha_3}{\alpha_1}=\frac{4[(3+\eta^2)/3]^{1/2}+[3K-1+\eta K']}{4[(3+\eta^2)/3]^{1/2}-[3K-1+\eta K']}, \qquad (11)$$

where

$$K=\sin^2\Theta[\cos^2\Phi Z_{a'}^2+\sin^2\Phi Z_c^2]+\cos^2\Theta Z_b^2$$
$$+\sin^2\Theta\sin2\Phi Z_{a'}Z_c,$$
$$K'=\sin^2\Theta[\cos^2\Phi(X_{a'}^2-Y_{a'}^2)+\sin^2\Phi(X_c^2-Y_c^2)]$$
$$+\cos^2\Theta(X_b^2-Y_b^2)+\sin^2\Theta\sin2\Phi(X_{a'}X_c-Y_{a'}Y_c).$$

The quantities $Z_{a'}$, Y_c, etc., in K and K' are just the direction cosines $\hat{z}\cdot\hat{a}'$, $\hat{y}\cdot\hat{c}$, etc.

For observation directions $\Theta=\Phi=0$ and $\Theta=\pi/2$, $0\leq\Phi\leq2\pi$, it can be shown from Eqs. (8), (9), and (10)

[14] G. T. Ewan, R. L. Graham, and J. S. Geiger, Nucl. Phys. **19**, 221 (1960).

[15] M. E. Rose, *Elementary Theory of Angular Momentum* (John Wiley and Sons, Inc., New York, 1957).
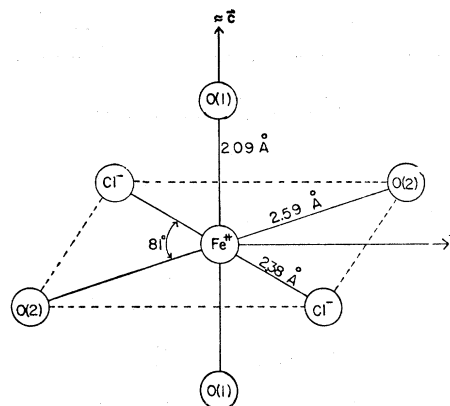
FIG. 3. Basic structural unit of the $FeCl_2\cdot4H_2O$ crystal. All angles are approximately equal to 90° except for the $Cl^--Fe^{++}-O(2)$ angle which is equal to 81°.

that $p_3(\theta_1,\phi_1)=p_3(\theta_2,\phi_2)$ and $p_1(\theta_1,\phi_1)=p_1(\theta_2,\phi_2)$. Consequently, for measurements in these directions, Eq. (11) is valid even in the presence of f' anisotropy since f' cancels out of Eq. (6) under these conditions. If we make the assumption that $(1+\eta^2/3)^{1/2}$ is approximately equal to one, since $(0\leq\eta<1)$, the area ratios for these special directions, obtained directly from Eq. (11), are

$$\frac{\alpha_3}{\alpha_1}(0,0)=\frac{3+b}{5-b},$$
$$\frac{\alpha_3}{\alpha_1}\left(\frac{\pi}{2},\Phi\right)=\frac{3+(a\cos^2\Phi+c\sin^2\Phi+d\sin2\Phi)}{5-(a\cos^2\Phi+c\sin^2\Phi+d\sin2\Phi)}, \qquad (12)$$

where

$$b=3Z_b^2+\eta(X_b^2-Y_b^2)=b(\eta,\alpha,\beta,\gamma),$$
$$a=3Z_{a'}^2+\eta(X_{a'}^2-Y_{a'}^2)=a(\eta,\alpha,\beta,\gamma),$$
$$c=3Z_c^2+\eta(X_c^2-Y_c^2)=c(\eta,\alpha,\beta,\gamma),$$
$$d=3Z_{a'}Z_c+\eta(X_{a'}X_c-Y_{a'}Y_c)=d(\eta,\alpha,\beta,\gamma).$$

Rather than solve these equations for η, α, β, and γ either analytically or with computer techniques, an approximate symmetry element associated with the crystal **c** axis was utilized to find the EFG parameters from the experimental data. This is described in the next section.

5. EXPERIMENTAL DATA AND EFG PARAMETERS

Previously it was mentioned that the ferrous ion is surrounded by a distorted octahedron composed of four water molecules and two chlorine ions. This octahedron is depicted in Fig. 3. It will be noted that there are actually two different sets of water molecules about the Fe^{++}, the set $O(2)$ being approximately one-half angstrom farther out that the set $O(1)$. [The nomenclature $O(1)$ and $O(2)$ is used since the x-ray data distinguish only the position of the oxygen atom in the

water molecules.] The O(1)-O(1) direction is approximately perpendicular to the plane formed by the two O(2)'s and the two Cl⁻'s and the O(2)-Fe⁺⁺-Cl⁻ angle is 81°. Therefore, the local electrostatic symmetry about the ferrous ion is approximately that due to a sixfold monoclinic coordination of negative ligands with the O(1)-O(1) direction corresponding to the monoclinic axis. We might expect therefore that the O(1)-O(1) direction (approximately parallel to the crystal c axis for both sites), would be a principal axis (either the major, minor, or intermediate) for the nuclear EFG.

Testing these possibilities in Eq. (12) and comparing with the experimental data appropriate to Eq. (12) [measurements (1)–(5) in Table I], a reasonable fit could be found only if one assumed the following:

(a) The c axis, assumed to be the O(1)-O(1) direction, is the minor axis of EFG. That is, $X_c=1$, $X_{a'}=X_b=Z_c=Y_c=0$.

(b) The major axis of the EFG, either ∥ or ⊥ to the Cl⁻-Cl⁻ direction, makes an angle of approximately 45° with respect to b. That is, $Z_b=Z_{a'}=\frac{1}{2}\sqrt{2}$.

(c) The ratio of the high-energy experimental absorption area to the low = α_H/α_L is equal to α_3/α_1 and not α_1/α_3. The high-energy absorption peak is the one occurring at $\approx+3$ mm/sec in Fig. 1.

(d) $\eta \approx 0.1$.

The EFG principal-axis system (PAS) proposed by (a) and (b) above, relative to the ferrous ion surroundings, is shown in Fig. 4. The PAS for the other site may be obtained by rotating the PAS shown through 180° about b. There is an indeterminacy remaining in the problem in that the PAS shown in Fig. 4 can go with either the upper or lower atomic configuration. That is, the major axis of the EFG is either parallel or perpendicular to the Cl⁻-Cl⁻ direction. This indeterminacy arises since the FeCl₂·4H₂O crystal has the two equivalent sites per unit cell.

Assumption (c) above implies that the energy of state $|\psi_3\rangle$ is greater than $|\psi_1\rangle$ and from Eq. (1), this implies that e^2qQ is positive. Since Q has been shown to be

FIG. 4. On the left is a view down the c axis of the crystal showing the atomic configuration in each site of the unit cell. The figure on the right indicates the position of the experimentally determined EFG principal axes in the ith site.

positive[16] and approximately equal to 0.29 b,[17] q is positive and may be calculated by substituting the measured splitting ΔE and $\eta=0.1$ into the expression $\Delta E=(e^2qQ/2)(1+\eta^2/3)^{1/2}$. (See Table I.)

Measurement (6) in Table I was made in order to determine if the fit obtained from measurements (1)–(5) was unique or merely one of many possible fits. If the assumption is correct that the c axis of the crystal is a principal axis of the EFG for both sites, then it may be shown from Eqs. (8), (9), and (10) that $p_3(\theta_1\phi_1)$
$=p_3(\theta_2\phi_2)$ for all measurements made in the (b−c) plane of the crystal (i.e., $0\le\Theta\le\pi$, $\Phi=\pi/2$). Under these conditions, as discussed in the previous section, Eq. (11) is valid even if f' is anisotropic. Therefore, using the EFG parameters defined by (a) through (d) above, the area ratio for direction 6 was calculated first from Eq. (11) and then compared and found to agree with the experimental ratio.

Measurements (8), for FeCl₂·4H₂O powder, indicate that f' is anisotropic at room temperature with the anisotropy diminishing as one goes to lower temperatures. In order to determine the effect of this anisotropy on a single-crystal area ratio, measurements (7) were made in a direction where f' anisotropy could be important; $(\Theta=\pi/4, \Phi=0)$. The comparison of the value calculated from Eq. (11), which assumes an isotropic f', with the experimental values, appears to support the powder data. That is, the f' anisotropy appears to diminish as one goes to lower temperatures since the area ratio calculated assuming f' is isotropic is closer to the low-temperature experimental ratio. Data of this type can provide meaningful information about this anisotropy provided the angular dependence of f' is known. In the harmonic approximation,[18] this angular

TABLE I. Single-crystal area ratios. Measured splitting and EFG parameters, assuming $Q=+0.29$ b: ΔE (300°K)=3.00 mm/sec, $\eta\approx0.1$, $\Rightarrow eq=+9.9\times10^{17}$ V/cm²; ΔE (77°K)=3.10 mm/sec; $\eta\approx0.1$, $\Rightarrow eq=+1.03\times10^{18}$ V/cm².

	Θ	Φ	300°K Expt. (α_H/α_L)	Calc. (α_3/α_1)	77°K Expt. (α_H/α_L)
(1)	0	0	1.21	1.25	1.29
(2)	$\pi/2$	0	1.24	1.25	1.26
(3)	$\pi/2$	$\pi/4$	0.82	0.89	
(4)	$\pi/2$	$-\pi/4$	0.87	0.89	
(5)	$\pi/2$	$\pi/2$	0.59	0.63	0.65
(6)	$\pi/4$	$\pi/2$	0.87	0.89	
(7)	$\pi/4$	0	1.44	1.25ᵃ	1.35
(8)	Powder		≈0.97	1.00ᵃ	$\gtrsim1.00$

ᵃ Calculated assuming an isotropic recoilless factor.

[16] C. E. Johnson, W. Marshall, and G. J. Perlow, Phys. Rev. 126, 1503 (1962).
[17] R. Ingalls, Phys. Rev. 133, A787 (1964).
[18] J. Petzold, Z. Physik 163, 71 (1961).

dependence is relatively simple and its substitution into the area ratio formula, Eq. (6), is straightforward.[19]

6. MAGNETIC SUSCEPTIBILITY

At this point, it is interesting to note that the single-crystal magnetic-susceptibility data[20] for $FeCl_2 \cdot 4H_2O$ indicate that the principal axes of the local susceptibility tensor do not coincide with the principal axes of the EFG tensor. The local monoclinic axis, O(1)-O(1), is a principal axis for both tensors as would be expected but in the plane perpendicular to the monoclinic axis, the principal axes have a relative orientation difference of $\approx 15°$. Although the susceptibility measurements were made in the 20–1°K temperature range and the Mössbauer data being compared was taken at 77°K, it does not seem plausible that a 15° variation could arise from the temperature difference. The fact that a 20°K measurement of an area ratio for one ferrous chloride sample showed no appreciable change from its 77°K value, argues in favor of this viewpoint. Consequently, the symmetry of the EFG interaction with the Fe^{57} nucleus is actually different than that of the susceptibility interaction of the paramagnetic ferrous ion. The difference may have its origin in core polarization effects although most probably, it is due to the fact that there is really no reason why they should be the same when the paramagnetic ion is in an electrostatic configuration of little or no symmetry. It might be noted that the samples used in both the Mössbauer and susceptibility measurements were in some cases from the same crystal, so that this symmetry difference is most likely quite real.

7. CONCLUSION

A method for adequately determining EFG parameters utilizing the Mössbauer technique has been presented. This method complements that used in nuclear quadrupole resonance in that it permits the evaluation of EFG's at nuclei which do not have ground-state quadrupole moments. An interesting experiment, comparing both methods, could be performed utilizing the Au^{197} nucleus, since it has a Mössbauer transition from a spin $\frac{1}{2}$, first excited state to a spin $\frac{3}{2}$ ground state.[21]

ACKNOWLEDGMENTS

The author is greatly indebted to Professor S. DeBenedetti and Dr. G. Lang for several helpful suggestions and criticisms during the course of this work. He is also indebted to Professor S. A. Friedberg and Dr. R. Ingalls for many stimulating discussions.

[19] P. Zory, Ph.D. thesis, Department of Physics, Carnegie Institute of Technology, 1964 (unpublished).

[20] J. T. Schriempf and S. A. Friedberg, Phys. Rev. 136, A518 (1964).

[21] L. D. Roberts and J. O. Thompson, Phys. Rev. 129, 664 (1963).

APPENDIX A

In deriving Eq. (8) for the relative absorption probabilities $p_3(\theta,\phi)$ and $p_1(\theta,\phi)$, we first consider the interaction of the nuclear quadrupole moment with the EFG. The Hamiltonian for the interaction is that given by Eq. (1a). Since H_Q does not commute with I_z, the general form for an eigenvector $|\psi_i\rangle$ of the system is

$$|\psi_i\rangle = \sum_{m=-3/2}^{3/2} C_{im}|\alpha', (I=\tfrac{3}{2}), m\rangle.$$

The letter m is the quantum number associated with the operator I_z while α' stands for any other quantum numbers necessary to specify the nuclear state.

It is easily shown that the eigenvectors associated with eigenvalues E_3 and E_1 are

$$
\begin{aligned}
E_3 &\to |\psi_3\rangle = \cos\rho|\alpha',\tfrac{3}{2},\tfrac{3}{2}\rangle + \sin\rho|\alpha', \tfrac{3}{2}, -\tfrac{1}{2}\rangle, \\
E_3 &\to |\psi_{-3}\rangle = \cos\rho|\alpha', \tfrac{3}{2}, -\tfrac{3}{2}\rangle + \sin\rho|\alpha',\tfrac{3}{2},\tfrac{1}{2}\rangle, \\
E_1 &\to |\psi_1\rangle = \sin\rho|\alpha',\tfrac{3}{2},\tfrac{3}{2}\rangle - \cos\rho|\alpha', \tfrac{3}{2}, -\tfrac{1}{2}\rangle, \\
E_1 &\to |\psi_{-1}\rangle = \sin\rho|\alpha', \tfrac{3}{2}, -\tfrac{3}{2}\rangle - \cos\rho|\alpha',\tfrac{3}{2},\tfrac{1}{2}\rangle,
\end{aligned}
\tag{13}
$$

where

$$
\cos\rho = [1 + (3/(3+\eta^2))^{1/2}]^{1/2}/\sqrt{2};
$$
$$
\sin\rho = [1 - (3/(3+\eta^2))^{1/2}]^{1/2}/\sqrt{2}.
$$

The two degenerate eigenvectors for the nuclear ground state are $|\alpha,\tfrac{1}{2},\tfrac{1}{2}\rangle$ and $|\alpha, \tfrac{1}{2}, -\tfrac{1}{2}\rangle$.

Since we are dealing with magnetic-dipole transitions,[14] the relative absorption probability for a transition, e.g., $|\alpha,\tfrac{1}{2},\tfrac{1}{2}\rangle$ to $|\psi_{-3}\rangle$, is given by (4); that is,

$$p_{\frac{1}{2},-3} = (|\hat{\theta}\cdot\langle\alpha,\tfrac{1}{2},\tfrac{1}{2}|\mathbf{M}|\psi_{-3}\rangle|^2 + |\hat{\phi}\cdot\langle\alpha,\tfrac{1}{2},\tfrac{1}{2}|\mathbf{M}|\psi_{-3}\rangle|^2),$$

where $\mathbf{M}$ is the nuclear magnetic dipole-moment operator. Since both degenerate ground states are equally populated and since only energetically different transitions are discriminated, the relative absorption probabilities p_3 and p_1 are given by

$$
\begin{aligned}
p_3 &= p_{\frac{1}{2}3} + p_{-\frac{1}{2},3} + p_{\frac{1}{2},-3} + p_{-\frac{1}{2},-3} = 2(p_{\frac{1}{2}3} + p_{-\frac{1}{2},3}), \\
p_1 &= p_{\frac{1}{2}1} + p_{-\frac{1}{2},1} + p_{\frac{1}{2},-1} + p_{-\frac{1}{2},-1} = 2(p_{\frac{1}{2}1} + p_{-\frac{1}{2},1}).
\end{aligned}
\tag{14}
$$

The reduction of terms in (14) is possible because of the symmetry in H_Q. Therefore, the expression for the kth relative absorption probability ($k=3$ or 1) is

$$
\begin{aligned}
p_k = 2(&|\hat{\theta}\cdot\langle\alpha,\tfrac{1}{2},\tfrac{1}{2}|\mathbf{M}|\psi_k\rangle|^2 + |\hat{\theta}\cdot\langle\alpha, \tfrac{1}{2}, -\tfrac{1}{2}|\mathbf{M}|\psi_k\rangle|^2 \\
&+ |\hat{\phi}\cdot\langle\alpha,\tfrac{1}{2},\tfrac{1}{2}|\mathbf{M}|\psi_k\rangle|^2 + |\hat{\phi}\cdot\langle\alpha, \tfrac{1}{2}, -\tfrac{1}{2}|\mathbf{M}|\psi_k\rangle|^2).
\end{aligned}
\tag{15}
$$

The matrix elements of $\mathbf{M}$ may be determined from the table found in Ref. (10), p. 63. Using these, the

quantities in Eq. (15) may be shown to be

$$|\hat{\theta}\cdot\mathbf{M}_{k\frac{1}{2}}|^2 = R^2\cos^2\theta[(A_k+B_k)^2\cos^2\phi$$
$$+(A_k-B_k)^2\sin^2\phi],$$

$$|\hat{\phi}\cdot\mathbf{M}_{k\frac{1}{2}}|^2 = R^2[(A_k+B_k)^2\sin^2\phi$$
$$+(A_k-B_k)^2\cos^2\phi],$$ (16)

$$|\hat{\theta}\cdot\mathbf{M}_{k,-\frac{1}{2}}|^2 = R^2 4B_k^2\sin^2\theta,$$

$$|\hat{\phi}\cdot\mathbf{M}_{k,-\frac{1}{2}}|^2 = 0,$$

where

$$A_3 = -(\sqrt{6})\cos\rho; \quad B_3 = \sqrt{2}\sin\rho,$$
$$A_1 = -(\sqrt{6})\sin\rho; \quad B_1 = -\sqrt{2}\cos\rho,$$

and

$$2R = \langle\alpha\tfrac{1}{2}\|M\|\alpha'\tfrac{3}{2}\rangle.$$

Substituting these results into Eq. (15) and utilizing the definitions of $\cos\rho$ and $\sin\rho$ as given by Eq. (13), one gets

$$p_3(\theta,\phi) = 2R[4[(3+\eta^2)/3]^{1/2}$$
$$+(3\cos^2\theta-1+\eta\sin^2\theta\cos2\phi)],$$
$$p_1(\theta,\phi) = 2R[4[(3+\eta^2)/3]^{1/2}$$
$$-(3\cos^2\theta-1+\eta\sin^2\theta\cos2\phi)].$$ (17)

Arbitrarily factoring out $2R$, the reduced matrix element, Eq. (17) becomes the expression for p_3 and p_1 given by Eq. (8) in the text.

Secondary-Electron Emission from Molybdenum Due to Positive and Negative Ions of Atmospheric Gases

P. Mahadevan, G. D. Magnuson, J. K. Layton,* and C. E. Carlston
General Dynamics/Convair, San Diego, California
(Received 30 June 1965)

Secondary-electron yields from a clean surface of Mo have been measured for H^+, H_2^+, H_3^+, H^-, O^+, O_2^+, O^-, O_2^-, N^+ and N_2^+ in the kinetic energy range 40 eV to 2 keV. These measurements have been made under ultrahigh vacuum of order 10^{-10} Torr. The rate of variation of the electron yield γ with kinetic energy of the incident ion decreases as the ion mass increases, consistently from H^+ to O_2^+. Evidence is presented to show that kinetic emission is much less affected by monolayer coverage of the surface than potential emissions is. For clean surfaces, the negative-ion yields represent most closely the kinetic-emission characteristics of the bombarding particles.

INTRODUCTION

ELECTRON-EMISSION efficiencies of positive ions of the rare gases bombarding a clean metal surface have been reported in an earlier publication from this laboratory.[1] The present measurements using atomic and molecular ions of hydrogen, nitrogen, and oxygen were undertaken to study the potential-energy dependence of the yields at low energies and the mass dependence of yields in the kinetic-emission range of energies. We have attempted to arrive at some qualitative conclusions regarding the effect of adsorbed gases on the target surface and the relative effects of gas coverage on potential and kinetic emission of electrons.

Electron emission due to positive-ion impact for various ion-target systems has been studied extensively. Due to impact of negative ions, electron emission can occur either by the ion releasing its extra electron into vacuum on impact with the surface or by kinetic ejection. Massey[2] suggests that among the reactions leading to the detachment of an electron from a negative ion, the most effective (in the absence of positive ions) is surface collision if the work function of the surface is greater than the electron affinity of the negative ion. In such a case a resonance transition of the extra electron from the negative ion (to an isoenergetic vacant level in the metal) is possible. The electron yields for negative ions were measured for all cases where the ions are stable. For clean surfaces, these yields represent most closely the kinetic-emission characteristics of the bombarding particles. No attempt has been made to estimate the contribution, if any, to the yield, of reflected negative ions or electrons detached from the negative ion and released into vacuum.

APPARATUS

The apparatus used for these measurements has been described in an earlier[1] publication. The background pressure is in the 10^{-10}-Torr range, the lowest so far recorded being 4×10^{-10} Torr. These low pressures have been achieved by continuous pumping for about a month. The operating pressure with source gas flowing and with the beam turned on did not exceed 2×10^{-9} Torr. The target-and-collector assembly has also been

* Now at General Atomic, A Division of General Dynamics Corporation, San Diego, California.
[1] P. Mahadevan, J. K. Layton, and D. B. Medved, Phys. Rev. 129, 79 (1963).
[2] H. S. W. Massey, *Negative Ions* (Cambridge University Press, Cambridge, England, 1950), p. 89.